Alzheimer disease and amyotrophic lateral sclerosis: An etiopathogenic connection

Xiaochuan Wang, M.D., Ph.D.[1,*], **Julie Blanchard, Ph.D.**[1], **Inge Grundke-Iqbal, Ph.D.**[1], **Jerzy Wegiel, D.V.M., Ph.D.**[2], **Han-Xiang Deng, M.D., Ph.D.**[3], **Teepu Siddique, M.D.**[3], and **Khalid Iqbal, Ph.D.**[1]

[1]Department of Neurochemistry, Inge Grundke-Iqbal Research Floor, New York State Institute for Basic Research, In Developmental Disabilities, Staten Island, NY 10314-6399, USA

[2]Department of Developmental Neurobiology, New York State Institute for Basic Research, In Developmental Disabilities, Staten Island, NY 10314-6399, USA

[3]Davee Department of Neurology and Clinical Neurological Sciences, Northwestern University Feinberg School of Medicine, Chicago, IL 60611, USA

Abstract

The etiopathogenesis of neither the sporadic form of Alzheimer disease (AD) nor of amyotrophic lateral sclerosis (ALS) are well understood. The activity of protein phosphatase-2A (PP2A), which regulates the phosphorylation of tau and neurofilaments, is negatively regulated by the myeloid leukemia-associated protein SET, also known as inhibitor-2 of PP2A, I_2^{PP2A}. In AD brain PP2A activity is compromised, probably because I_2^{PP2A} is overexpressed and is selectively cleaved at asparagine 175 into an N-terminal fragment, I_{2NTF}, and a C-terminal fragment, I_{2CTF}, and both fragments inhibit PP2A. Here we analyzed the spinal cords from ALS and control cases for I_2^{PP2A} cleavage and PP2A activity. As observed in AD brain, we found a selective increase in the cleavage of I_2^{PP2A} into I_{2NTF} and I_{2CTF} and inhibition of the activity and not the expression of PP2A in the spinal cords of ALS cases. To test the hypothesis that both AD and ALS could be triggered by I_{2CTF}, a cleavage product of I_2^{PP2A}, we transduced by intracerebroventricular injections newborn rats with adeno-associated virus serotype 1 (AAV1) containing human I_{2CTF}. AAV1- I_{2CTF} produced reference memory impairment and tau pathology, and intraneuronal accumulation of Aβ by 5–8 months, and motor deficit and hyperphosphorylation and proliferation of neurofilaments, tau and TDP-43 pathologies, degeneration and loss of motor neurons and axons in the spinal cord by 10–14 months in rats. These findings suggest a previously undiscovered etiopathogenic relationship between sporadic forms of AD and ALS that is linked to I_2^{PP2A} and the potential of I_2^{PP2A}-based therapeutics for these diseases.

Keywords

Alzheimer's disease; amyotrophic lateral sclerosis; Guam Parkinsonism dementia complex; protein phosphatase-2A; inhibitor-2 of protein phosphatase-2A; I_2^{PP2A}/SET; abnormal hyperphosphorylation of tau

Corresponding Author: Khalid Iqbal, Ph.D., Chairman, Department of Neurochemistry, New York State Institute for Basic Research in Developmental Disabilities, 1050 Forest Hill Road, Staten Island, NY 10314-6399, USA, Phone: 1-718-494-5259; Fax: 1-718-494-1080, khalid.iqbal.ibr@gmail.com.
Present Address: Pathophysiology Department, Tongji Medical College, Huazhong University of Science & Technology, Wuhan, Hubei, P.R. China

Introduction

Alzheimer disease (AD), amyotrophic lateral sclerosis (ALS), and Guam Parkinsonism dementia complex (PDC) are all chronic progressive neurodegenerative disorders of the central nervous system seen in middle- to old-aged individuals. AD alone affects over five million individuals in the United States and over thirty-five million worldwide. ALS, also known as Lou Gehrig's disease, is estimated to affect over 350,000 individuals world, including ~20,000 Americans with 5,000 new cases each year (NINDS ALS Information). PDC, which frequently occurs as ALS/PDC, is highly prevalent in the native Chamorro population of Guam [16,17].

Neurodegeneration in AD is characterized by the presence of numerous intraneuronal neurofibrillary tangles made up of paired helical filaments or ~15 nm straight filaments, and extracellular Aβ deposits in neuritic (senile) plaques in the brain, especially the hippocampus and the neocortex. In AD, the neurofibrillary pathology is also seen as neuropil threads and in dystrophic neurites surrounding the plaque Aβ core. The neurofibrillary changes in AD as well as in a family of related neurodegenerative disorders called tauopathies, are made up of microtubule associated protein tau in an abnormally hyperphosphorylated state [14,15]. These tauopathies include PDC, fronto-temporal dementia linked to chromosome 17 caused by mutations in the tau gene (FTDP-17 tau), Pick disease, corticobasal degeneration, and progressive supranuclear palsy (PSP). In all these tauopathies, neurofibrillary degeneration is associated with functional impairment, i.e., cognitive impairment in tauopathies involving lesions in the forebrain, and motor impairment in PSP, where the lesions are mainly in the brain stem and spinal cord.

ALS primarily involves degeneration of the motor neurons in the spinal cord that is associated with muscle weakness and atrophy, followed by loss of function throughout the body. The key pathological marker of ALS includes aggregated phosphorylated neurofilaments trapped in ubiquitin-, p-62-, TDP-43-, and ubiquilin2-positive aggregates of skein-like, stellate, and globular or lewy-like inclusions. Moreover, ALS is also characterized by a proliferation and aggregation of phosphorylated neurofilaments in the cytoplasm of motor neurons and large myelinated axons of the anterior and lateral corticospinal tracts of the spinal cord. ALS/PDC induces severe cortical atrophy and both neurofibrillary degeneration of the AD type in the brain and of motor neurons in the spinal cord [25,17]. Clinically, ALS/PDC shows both AD and ALS phenotypes, i.e., progressive dementia, extrapyramidal symptoms, and signs of lower and upper motor neuron dysfunction [16].

Less than 1% of AD cases are familial and are caused by point mutations in the genes encoding amyloid precursor protein, presenilin-1 or presenilin-2. In the case of ALS, as many as 10% of the cases are familial and the adult-onset disease is caused by point mutations in superoxide dismutase 1 (SOD1), TAR DNA-binding protein (TARDP) encoding TDP-43, fused in sarcoma (FUS), and ubiquilin2 genes [5,6,19,28,32] and a hexanucleotide repeat expansion in an intron of C9ORF72 [4,26]. However, to date neither the exact etiopathogenesis of the sporadic form of AD nor of sporadic ALS are well understood. In the case of ALS/PDC, environmental toxins such as β-methylamino-L-alanine (BMAA) that could affect the activities of several protein kinases and phosphatases have been suspected but not experimentally demonstrated [8].

Hyperphosphorylation of tau and neurofilaments at serine/threonine residues leads to their aggregation [15,1,29]. The activity of protein phosphatase-2A (PP2A), which regulates the phosphorylation of tau and neurofilaments [9,12,33] and accounts for ~70% of the human brain phosphoseryl/phosphothreonyl phosphatase activity [21], is negatively regulated by

the myeloid leukemia-associated protein SET, also known as inhibitor-2 of PP2A, I_2^{PP2A} [20].

In AD brain the PP2A activity is compromised and is believed to be a cause of the abnormal hyperphosphorylation of tau [10,11,18]. I_2^{PP2A}, a 277 amino acid full-length nuclear protein, is cleaved at aspargine 175 into an amino terminal fragment, I_{2NTF}, and a C-terminal fragment, I_{2CTF}, and translocated from the neuronal nucleus to the cytoplasm where it co-localizes with PP2A and abnormally hyperphosphorylated tau [31]. Both I_{2NTF} and I_{2CTF} interact with the PP2A catalytic subunit PP2Ac and inhibit the phosphatase activity [2]. Here we report (1) that like in AD brain, I_2^{PP2A} is cleaved into I_{2NTF} and I_{2CTF} and PP2A activity is compromised in the spinal cords of ALS cases, and (2) that AAV1-mediated expression of I_{2CTF} in the central nervous system produces AD-, and ALS-, like pathologies and associated cognitive and motor impairments in rats.

Materials and Methods

ALS and Control Tissue

Frozen autopsied spinal cord samples from ten clinically- and histopathologically-confirmed cases of sporadic ALS and three control cases (sTable 1) were obtained from the ALS Autopsy Retrieval Program at Northwestern University Feinberg School of Medicine (NUFSM) funded by the Les Turner ALS Foundation. The spinal cords were employed to study the level and activity of PP2A, and the cleavage of I_2^{PP2A} into I_{2NTF} and I_{2CTF}.

Animals and Intracerebroventricular (ICV) Injection of AAV

Normal Wistar rats were purchased from Charles River Laboratories (Wilmington, MA) and bred and maintained in the New York State Institute for Basic Research Animal Colony. On the day of birth, designated as P 0.5, pups were individually cryoanesthetized on ice for 5 min, and 2 μl of AAV1-I_{2CTF} was injected into each lateral ventricle using a specially designed, fine 10 μl Hamilton syringe equipped with a 30G/0.5 inch/hypodermic cemented needle (Hamilton Syringe Company, Reno, NV). A total of 8×10^9 AAV1 genomic equivalents in 4 μl were injected intracerebroventricularly into each rat. Control animals were treated identically except that they received vector only, i.e., AAV1-GFP. Animals were housed in a facility maintained at 23°C with a light/dark cycle of 12 hours (lights off at 6:00 p.m.) and with access to food and water *ad libitum*. Behavioral studies included 7 AAV1-GFP and 8 AAV1-I_{2CTF} infected animals. Immunohistochemical and Western blot analysis employed three animals/group.

All procedures carried out on animals were conducted in compliance with NIH guidelines and protocols approved by our institutional Animal Welfare Committee.

Perfusion and Tissue Processing

I_{2CTF} and GFP rats were transcardially perfused with 100 mM phosphate buffered saline. The left half of the brain and 5 mm long segments from the cervical, thoracic and lumbar regions of the spinal cord were immersion-fixed in 4% paraformaldehyde for histological and immunohistochemical studies. Two 3 mm segments from the cervical, thoracic and lumbar regions of the spinal cord were immersion fixed in 2.5% buffered glutarldehyde, postfixed with osmium, embedded in Epon, cut into semi- and ultra-thin sections, and examined by light and electron microscopies. The right half of each brain was dissected into hippocampus, cerebral cortex, subcortical area, and the cerebellum, and frozen on dry ice until used for biochemical studies.

Image analysis and semiquantification of immunofluorescence

The sections were examined using a confocal microscope (PCM 2000 Confocal Imaging System, Nikon, Melville, NY) and images were acquired for quantitative analysis using a 40x objective. The area of interest was outlined and maximum projection images were generated based on confocal z-stacks. The antibody staining was semi-quantitated by measuring the mean fluorescence intensities (MFIs) using NIH Image J software. Six to ten images of the tissue sections from 3 animals/group stained for MAP2, synaptophysin or synapsin 1 were obtained per hippocampal CA1 and CA3 regions, respectively. MFI per square micrometer area was calculated by dividing the MFI units by the area of the outlined regions.

Quantitation of loss of motor neurons and neurofilament and ubiquitin immunostaining

The number of Nissl-stained motor neurons was counted and calculated from a total number of 21 tissue sections from 3 animals per group.

The immunostaining with SM133, SM134 and ubiquitin was quantitated by measuring the mean optical density (MOD) using Image-Pro Plus Version 6.0 (Media Cybernetics, Inc., MD, USA). Images of the tissue sections, 21 in total, from 3 animals/group were obtained from spinal cords at lumbar level. MOD per square micrometer was calculated by dividing the MOD units by the area of the outlined regions.

Quantitation of the density of Purkinje cells

The cerebellum from one half of the brain fixed in paraformaldehyde and saved for histology was paraffin-embedded. The 8 μm sections of the paraffin-embedded tissue stained with cresyl violet were used for quantification of the Purkinje cells. The number of Purkinje cells was determined as numerical density of cells per mm of the border between granule cell layer and molecular layer of the cerebellar cortex. More than 20 test areas were examined using objective lens 20x. Cells were counted using support of the Stereoinvestigator program (Microbrightfield).

Other Methods

See Supplementary Information for the construction of recombinant plasmids, vector packaging and titering, Western blots, extraction of sarkosyl insoluble tau, immunoprecipitation, PP2A activity assay, immunohistochemistry and toluidine blue staining, Fluor-Jade B labeling, Morris water maze spatial reference memory task and neurological examination.

Statistical Analysis

Data were analyzed with SPSS 12.0 statistical software. The one-way analysis of variance procedure followed by least significant difference post hoc tests were used to determine the statistical significance of differences of the means. To analyze the correlations among variables, Pearson correlations were computed with bivariate correlations procedure. Mann-Whitney U-test was used for assessment of the difference between the groups for neurological examination. The data on spatial reference memory tasks were analyzed using Main-Effects ANOVA. The difference in the density of Purkinje cells between GFP and I_{2CTF} rats was analyzed by t-test. Statistical significance was accepted at the 95% confidence level ($p < 0.05$). Data were expressed as mean ± SEM.

Results

I_2^{PP2A} is cleaved into I_{2NTF} and I_{2CTF} and PP2A activity is compromised in the spinal cords of ALS cases

Aggregation of hyperphosphorylated neurofilaments in the spinal cord is a part of ALS pathology and PP2A is known to be the major regulator of the phosphorylation of neurofilaments [35,12]. We investigated if, as previously noted in AD brain, the inhibition of PP2A and resulting cleavage of I_2^{PP2A} into I_{2NTF} and I_{2CTF} was also involved in the neurofilament pathology in ALS. We determined the levels of I_{2NTF} and I_{2CTF} and the level and activity of PP2A in the spinal cords of ALS and control cases (sTable 1) by Western blots. We found a selective increase in the levels of I_{2NTF} (Fig. 1b) and I_{2CTF} (Fig. 1d) and a decrease in the activity but not the level of PP2A in the spinal cords of ALS cases, suggesting the possible involvement of I_2^{PP2A} cleavage-mediated inhibition of PP2A activity in this disease (Fig. 1).

Chronic adeno-associated virus-mediated expression of I_{2CTF} in the central nervous system results in the inhibition of PP2A activity, both in the spinal cord and the brain in rats

To test whether the cleavage of I_2^{PP2A} can lead to AD, ALS, and ALS/PDC-like pathologies and functional impairments, a plasmid containing I_{2CTF} and enhanced green fluorescent protein (GFP) or, as a control, GFP alone, were packaged into recombinant AAV serotype 1 and the virus purified and titered. On the day of birth, Wistar rat pups were individually cryoanesthetized on ice, then received bilateral intracerebroventricular (ICV) injection (2x2 μl containing a total of 8 x 10^9 AAV1 genomic equivalents) of AAV1-I_{2CTF}/GFP or, as a control, AAV1-GFP, (Fig. 2a). These animals showed neuronal transduction both in the brain and the spinal cord at 14 months post-AAV1 infection, as determined by immunohistochemical staining with anti-GFP (Fig. 2b). Western blots developed with a rabbit polyclonal antibody to I_{2CTF} showed an increase in I_{2CTF} expression in the brains of I_{2CTF} as compared with the GFP control animals; the level of I_{2CTF} was only a fraction of that of I_2^{PP2A} but the ratio of I_{CTF} to full-length I_2^{PP2A} was considerably increased in I_{2CTF} rats (Fig. 2c). AAV1-I_{2CTF} had no detectable effect on the expression of the catalytic subunit PP2Ac but markedly reduced the phosphatase activity in rat spinal cord and brain (Fig. 2d, e).

AAV1-I_{2CTF} rats show reference memory impairment and motor function deficit

To study whether the I_{2CTF} rats displayed any clinical phenotypes of AD and ALS, we tested them for reference memory as a measure of cognitive performance and hind limb extension reflex, beam walking test and prehensile traction test as measures of locomotivity; the animals were too heavy and suffered hind limb paralysis to be tested successfully for Rotarod test. I_{2CTF} rats showed deficits in spatial reference memory at 5 months and 8 months of age in Morris water maze task, and in long-term memory when tested one month after the previous water maze training (Fig. 3a, b). Both groups of animals learned to find the hidden platform from day 1 to day 2 but the performance of the I_{2CTF} animals remained lower than the control rats throughout the training, suggesting a memory impairment. The lower performance of I_{2CTF} rats than the control animals three months later and then in transfer test further after one month suggests that the memory deficit was probably the result of difficulties in information retrieval; memory is a cognitive process that includes encoding, consolidation and retrieval. The I_{2CTF} rats showed long-term memory impairment since the consolidation processes of the information extended 24 hours or more in the above spatial reference memory protocol. Analysis of the water maze data in fractional time in platform quadrant or the number of platform crossings did not show any significant differences between I_{2CTF} and GFP rats, suggesting that the impairment in the I_{2CTF} rats in finding the

hidden platform was unlikely due to any physical or motivational deficit which could have affected the first several seconds' performance compared to the later test period. Collectively the I_{2CTF} rats showed deficits in hippocampal-dependent cognitive performance and in reactivation of the long-term memory trace of spatial information.

Up until ~9 months both I_{2CTF} and GFP rats showed no apparent physical signs of neurological impairment. However, starting at ~10–12 months the I_{2CTF} but not the GFP control animals showed atrophy and hind leg dragging which got progressively worse, developing into moderate paralysis by 14 months. The I_{2CTF} rats had a significantly impaired neurological response, as determined by a total neuroscore (sTable 2) which was based on various measures of sensory motor functions, muscular strength and general neurological response (Fig. 3c, Mann-Whitney U-Test, p = 0.006). The I_{2CTF} animals displayed abnormal posture and clasping of the hind limb when elevated by the tail (Fig. 3d). Unlike the GFP control rats, the I_{2CTF} rats were unable to hold themselves with their forelimbs on a rod (Fig. 3e; Movies S1, S2) and were unable to walk on a 4 cm flat elevated beam (Fig. 3f; Movies S3, S4).

AAV1-I_{2CTF} rats show ALS-type pathology in the spinal cord and AD-type changes in the brain

Histological examination of the spinal cords of the 14-month-old I_{2CTF} rats revealed major features of ALS-type neurodegeneration. Nissl stained paraffin sections of spinal cords showed a loss of motor neurons in I_{2CTF} as compared to the GFP control rats (Fig. 4a–g). In the I_{2CTF} rats, the motor neurons in the cervical and the thoracic regions of the spinal cord displayed shrinkage and condensation, resulting in expansion of pericellular space (Fig. 4b, d). The lumbar segment revealed spongy changes and motor neurons with marked vacuolization (Fig. 4f). Toluidine blue stained semi-thin sections of the Epon-embedded spinal cords revealed different stages of axonal swelling and degeneration with condensation of the axoplasm in I_{2CTF} rats (Fig. 4h, i). More advanced degeneration was seen in the lateral bundles, including necrosis of the axons with accumulation of cellular debris (Fig. 4i). Electron microscopic examination revealed marked proliferation, aggregation and condensation of neurofilaments into bundles in the motor neuron cytoplasm and processes, especially prominent in the myelinated axons, and myelin sheath loss in the spinal cords of the I_{2CTF} rats (Fig. 4j, k). Moreover, in I_{2CTF} animals, between aggregates of neurofilaments, compact fibrous bundles (CFB) of ~20–35 nm wide filaments were observed. They were either straight or they had a serpentine shape, and they were up to several microns long (Fig. 4l, m). The CFBs were too tightly packed to reveal their fine structural details. These pathological changes were seen in non-myelinated fibers at all three levels, i.e., cervical, thoracic, and lumbar, of the spinal cord.

Toluidine blue staining of the paraffin sections of the cerebellum showed that expression of I_{2CTF} in the rat CNS caused selective shrinkage and condensation of Purkinje cell cyto- and nucleo-plasm and focal severe loss of these cells (Fig. 4n–q); quantitation of the numerical density of Purkinje cells in cresyl violet stained paraffin sections of the cerebellum showed a highly significant (p<0.001) decrease in I_{2CTF} (7.6 cells/mm) as compared with GFP control (15.7 cells/mm) animals (Fig. 4r). Although Purkinje cells are relatively spared from degeneration in AD, cerebellar degeneration is common to several other progressive degenerative disorders.

In agreement with the Nissl staining (Fig. 4a–g), immunohistochemical staining with monoclonal antibody SMI33 to non-phosphorylated neurofilaments in sections counterstained with hematoxylin showed a fewer number of motor neurons in the spinal cord from I_{2CTF} as compared with GFP control rats (Fig. 5a). Immunohistochemical staining with monoclonal antibody SMI34 to phosphoneurofilaments showed a proliferation of

phosphoneurofilaments in motor neurons and axonal fiber tracts in the spinal cords of I_{2CTF} animals (Fig. 5g–l). Furthermore, consistent with the aggregation of neurofilaments seen by electron microscopy, the SMI34 immunostaining was punctated (Fig. 5h, j, l). These findings suggested that the ALS type pathology in the I_{2CTF} rats could be due to the inhibition of PP2A and consequent hyperphosphorylation of neurofilaments.

Since PP2A is the major tau phosphatase [21] and neurofibrillary degeneration of abnormally hyperphosphorylated tau has been reported in PDC and ALS/PDC[23,24], we carried out immunohistochemical staining for abnormally phosphorylated tau on the spinal cords of I_{2CTF} and GFP rats. Perikarya of motor neurons from I_{2CTF} and not GFP control rats showed immunostaining with a rabbit polyclonal phosphoserine 262 tau antibody (Fig. 5m-r). The pSer262 tau antibody stained occasional plaque-like (Fig. 5n) and tangle-like (Fig. 5p) structures and revealed aggregated hyperphosphorylated tau (Fig. 5r) in the motor neurons of the I_{2CTF} rats.

Consistent with proliferation and aggregation of hyperphosphorylated neurofilaments, the ubiquitin staining was axonal and was markedly higher in I_{2CTF} than GFP control rat spinal cords (Fig. 5s, t; sFig 1). TDP-43 immunohistochemistry revealed an abnormal condensation, forming skein-like inclusions and translocation of the protein from the nucleus to the cytoplasm in the motor neurons of the I_{2CTF} rat spinal cords (Fig. 5u, v).

Since the phosphatase activity was reduced in the brains of I_{2CTF} rats (Fig. 2e) and these animals showed cognitive impairment (Fig. 3a, b), we investigated the hyperphosphorylation of tau in the brain. Consistent with our previous study[34] which showed tau pathology and intraneuronal $A\beta$ in 8-month I_{2CTF} rats, we found a marked increase in abnormal hyperphosphorylation of tau in the 14-month-old I_{2CTF} rat brain (Fig. 6a–c). This abnormal hyperphosphorylation of tau in the I_{2CTF} rats resulted in a marked increase in sarkosyl insoluble tau and a small decrease in total tau (Fig. 6d). The decrease in the total tau reflects neurodegeneration in the I_{2CTF} rats.

Fluorojade B histochemical staining, a sensitive marker of neurodegeneration confirmed an increase in neurodegeneration in the I_{2CTF} rats (Fig. 7a, b). Consistent with Fluorojade B staining, the level of neuron-specific βIII tubulin was decreased in I_{2CTF} animals (Fig. 7c). Furthermore, a decrease in the dendritic and synaptic plasticity was observed by immunohistochemical staining and by Western blots developed with anti-MAP2 and anti-synapsin 1/anti-synaptophysin, respectively, in the I_{2CTF} rats (Fig. 7d–f). The I_{2CTF} rats not only showed extensive tau pathology and neurodegeneration but also showed intraneuronal accumulation of βAPP, $A\beta_{1-40}$ and $A\beta_{1-42}$ in the brain (Fig. 8a–c).

Discussion

The activity of PP2A which regulates the phosphorylation of both tau and neurofilaments is in turn regulated by I_2^{PP2A}. I_2^{PP2A}, primarily a nuclear protein, is cleaved into I_{2NTF} and I_{2CTF} by asparaginyl endopeptidase under conditions of acidosis such as following ischemia, and translocates from the neuronal nucleus to the cytoplasm where it binds to PP2A catalytic subunit PP2Ac and inhibits its activity [22,2,3]. Previously we reported a selective increase in the cleavage and translocation of I_2^{PP2A} from the neuronal nucleus to the cytoplasm and a decrease in PP2A activity in AD brain [31]. Increase in the levels of I_{2NTF} and I_{2CTF} and decrease in PP2A activity in spinal cords of ALS cases found in the present study thus suggested an etiopathogenic mechanism of ALS that is similar to that of AD.

PP2A activity is tightly regulated in the cell and knocking out of this phosphatase in the brain of transgenic mice is lethal [13]. In the present study, a small persistent decrease in PP2A activity on a chronic basis induced by $SET\alpha/I_{2CTF}$ in rat CNS, produced both AD

type and ALS type pathological changes. PP2A and SET/I_2^{PP2A} are normally expressed both in the brain and in the spinal cord gray matter[30]. In the present study, the AD-like changes in tau and Aβ, neurodegeneration and cognitive impairment, preceded the ALS-like disease, i.e., axonal swelling and degeneration with condensation of the axoplasm and loss of myelin, degeneration of motor neurons associated with proliferation, aggregation and condensation of neurofilaments into bundles, and TDP-43-like inclusions and translocation of the protein from the neuronal nucleus to the cytoplasm in the spinal cord, and motor impairment. This time sequence of pathology and clinical phenotype was probably mainly due to the fact that the rat pups were infected ICV with AAV1-$I_{2CTF/GFP}$, which probably resulted in an earlier transduction and/or a faster rate of neurodegeneration in the forebrain than in the cerebellum and the spinal cord. We observed the AAV1-induced expression of I_{2CTF} both in the brain and in the spinal cord in rats. Whether some of the pathology merely spread from the brain to the spinal cord with time in the AAV1-I_{2CTF}-GFP rats, though less likely, cannot be ruled out. The robust transduction of choroid plexus was probably due to ICV injection of the virus, which our previous study showed to occur as early as three weeks post-infection [34]. However, the motor deficit and the loss of motor neurons in the spinal cord of I_{2CTF} rats in the present study was observed at 10–14 months. Nevertheless, we cannot rule out the possible involvement of the disruption of the choroid plexus epithelial cells in the neurodegeneration of the motor neurons in the spinal cord.

Traumatic brain injury (TBI), especially of the hind brain associated with football, boxing, and baseball, has often been confused with ALS, probably because of the shared disease mechanisms. The cerebellum and Purkinje cell layer are especially rich in PP2A and I_2^{PP2A} [30]. Degeneration of the Purkinje cells in the I_{2CTF} rats observed in the present study is consistent with a high vulnerability of this brain area to injury. TBI-induced ischemic stroke due to acidosis probably results in the release of asparagine endopeptidase (AEP), also known as legumain, from the lysosomes that cleaves I_2^{PP2A} at asparagine 175 into I_{2NTF} and I_{2CTF}, as has been shown in an experimentally-induced middle cerebral artery occlusion mouse model[22]. Both I_{2NTF} and I_{2CTF}, because of their small sizes, translocate from the neuronal nucleus to the cytoplasm and bind to the catalytic subunit of PP2A, PP2Ac, and inhibit the phosphatase activity[2]. PP2A is known to regulate the activities of several tau and neurofilament protein kinases which include calcium, calmodulin-dependent protein kinase II, protein kinase A, glycogen synthase kinase-3β, ERK1/2, MEK1/2, and p70S6 kinase[18]. Inhibition of PP2A probably leads to hyperphosphorylation and aggregation of tau and neurofilaments, both directly and by enhancing the activities of several kinases. The cleavage and translocation of I_2^{PP2A} from the neuronal nucleus to the cytoplasm could also have caused neurodegeneration due to the loss of the protection normally provided by the full-length protein as an inhibitor of DNase and a protector of acetylation of histones[7,27]. The decrease in PP2A activity and the activation of several protein kinases regulated by the phosphatase could also be involved in the promotion of the phosphorylation of I_2^{PP2A} at Ser9 that stabilizes its location in the neuronal cytoplasm by inactivation of its nuclear localization signal [6]AKVSKK[11] [36]. Acidosis of the CNS following ischemia and hypoxia can both lead to activation and translocation of AEP from neuronal lysosomes to the cytoplasm [3]. In the neuronal cytoplasm the activated AEP can then cleave I_2^{PP2A} at asparagine 175 into I_{2NTF} (amino acid residues 1–175) and I_{2CTF} (amino acid residues 176-277) and which, because of their small sizes, easily diffuse between the nucleus and the cytoplasm [31,22,3]. Thus, depending on the location of the ischemic and hypoxic changes in the CNS, the resulting acidosis in the brain can lead to AD-like and in the spinal cord to ALS-like pathology, and injury to the cerebellum accordingly can result in the degeneration of the Purkinje cells.

In short, the sporadic forms of AD and ALS represent most of the cases with these diseases. Less than 1% of AD and 10% of ALS cases are familial. In AD brain PP2A activity is

compromised and a selective increase in the cleavage of I_2^{PP2A} into I_{2NTF} and I_{2CTF} is believed to be a cause of this inhibition and the subsequent abnormal hyperphosphorylation of tau [10,11,31]. The discoveries of the increase in the spinal cord levels of I_{2NTF} and I_{2CTF} and a decrease in PP2A activity in ALS and the generation of both AD- and ALS-type pathologies with the expression of I_{2CTF} in rat in the present study suggests that an I_2^{PP2A}/PP2A-based therapy could succeed in inhibiting AD, ALS and related conditions. AAV1-I_{2CTF} rats which reproduced some of the key histopathological and clinical features of both AD and ALS could be used for drug development in preclinical studies.

Supplementary Material

Refer to Web version on PubMed Central for supplementary material.

Acknowledgments

References

1. Alonso A, Zaidi T, Novak M, Grundke-Iqbal I, Iqbal K. Hyperphosphorylation induces self-assembly of tau into tangles of paired helical filaments/straight filaments. Proc Natl Acad Sci USA. 2001; 98 (12):6923–6928. [PubMed: 11381127]

2. Arnaud L, Chen S, Liu F, Li B, Khatoon S, Grundke-Iqbal I, Iqbal K. Mechanism of inhibition of PP2A activity and abnormal hyperphosphorylation of tau by I(2)(PP2A)/SET. FEBS Lett. 2011; 585 (17):2653–2659. [PubMed: 21806989]

3. Basurto-Islas G, Grundke-Iqbal I, Tung YC, Liu F, Iqbal K. Activation of Asparaginyl Endopeptidase Leads to Tau Hyperphosphorylation in Alzheimer's Disease. J Biol Chem. 2013; 288:17495–17507.10.1074/jbc.M112.446070 [PubMed: 23640887]

4. DeJesus-Hernandez M, Mackenzie IR, Boeve BF, Boxer AL, Baker M, Rutherford NJ, Nicholson AM, Finch NA, Flynn H, Adamson J, Kouri N, Wojtas A, Sengdy P, Hsiung GY, Karydas A, Seeley WW, Josephs KA, Coppola G, Geschwind DH, Wszolek ZK, Feldman H, Knopman DS, Petersen RC, Miller BL, Dickson DW, Boylan KB, Graff-Radford NR, Rademakers R. Expanded GGGGCC hexanucleotide repeat in noncoding region of C9ORF72 causes chromosome 9p-linked FTD and ALS. Neuron. 2011; 72 (2):245–256.10.1016/j.neuron.2011.09.011 [PubMed: 21944778]

5. Deng HX, Chen W, Hong ST, Boycott KM, Gorrie GH, Siddique N, Yang Y, Fecto F, Shi Y, Zhai H, Jiang H, Hirano M, Rampersaud E, Jansen GH, Donkervoort S, Bigio EH, Brooks BR, Ajroud K, Sufit RL, Haines JL, Mugnaini E, Pericak-Vance MA, Siddique T. Mutations in UBQLN2 cause dominant X-linked juvenile and adult-onset ALS and ALS/dementia. Nature. 2011; 477 (7363): 211–215.10.1038/nature10353 [PubMed: 21857683]

6. Deng HX, Hentati A, Tainer JA, Iqbal Z, Cayabyab A, Hung WY, Getzoff ED, Hu P, Herzfeldt B, Roos RP, et al. Amyotrophic lateral sclerosis and structural defects in Cu,Zn superoxide dismutase. Science. 1993; 261 (5124):1047–1051. [PubMed: 8351519]

7. Fan Z, Beresford PJ, Oh DY, Zhang D, Lieberman J. Tumor suppressor NM23-H1 is a granzyme A-activated DNase during CTL-mediated apoptosis, and the nucleosome assembly protein SET is its inhibitor. Cell. 2003; 112 (5):659–672. [PubMed: 12628186]

8. Garruto RM. Pacific paradigms of environmentally-induced neurological disorders: clinical, epidemiological and molecular perspectives. Neurotoxicology. 1991; 12 (3):347–377. [PubMed: 1745428]

9. Gong CX, Lidsky T, Wegiel J, Zuck L, Grundke-Iqbal I, Iqbal K. Phosphorylation of microtubule-associated protein tau is regulated by protein phosphatase 2A in mammalian brain. Implications for

neurofibrillary degeneration in Alzheimer's disease. J Biol Chem. 2000; 275 (8):5535–5544. [PubMed: 10681533]

10. Gong CX, Shaikh S, Wang JZ, Zaidi T, Grundke-Iqbal I, Iqbal K. Phosphatase activity toward abnormally phosphorylated tau: decrease in Alzheimer disease brain. J Neurochem. 1995; 65 (2): 732–738. [PubMed: 7616230]

11. Gong CX, Singh TJ, Grundke-Iqbal I, Iqbal K. Phosphoprotein phosphatase activities in Alzheimer disease brain. J Neurochem. 1993; 61 (3):921–927. [PubMed: 8395566]

12. Gong CX, Wang JZ, Iqbal K, Grundke-Iqbal I. Inhibition of protein phosphatase 2A induces phosphorylation and accumulation of neurofilaments in metabolically active rat brain slices. Neurosci Lett. 2003; 340 (2):107–110. [PubMed: 12668248]

13. Gotz J, Schild A. Transgenic and knockout models of PP2A. Methods Enzymol. 2003; 366:390–403. [PubMed: 14674263]

14. Grundke-Iqbal I, Iqbal K, Quinlan M, Tung YC, Zaidi MS, Wisniewski HM. Microtubule-associated protein tau. A component of Alzheimer paired helical filaments. J Biol Chem. 1986; 261 (13):6084–6089. [PubMed: 3084478]

15. Grundke-Iqbal I, Iqbal K, Tung YC, Quinlan M, Wisniewski HM, Binder LI. Abnormal phosphorylation of the microtubule-associated protein tau (tau) in Alzheimer cytoskeletal pathology. Proc Natl Acad Sci USA. 1986; 83 (13):4913–4917. [PubMed: 3088567]

16. Hirano A, Kurland LT, Krooth RS, Lessell S. Parkinsonism-dementia complex, an endemic disease on the island of Guam. I. Clinical features. Brain. 1961; 84:642–661. [PubMed: 13907609]

17. Hirano A, Malamud N, Kurland LT. Parkinsonism-dementia complex, an endemic disease on the island of Guam. II. Pathological features. Brain. 1961; 84:662–679. [PubMed: 13907610]

18. Iqbal K, Alonso A, Chen S, Chohan MO, El-Akkad E, Gong CX, Khatoon S, Li B, Liu F, Rahman A, Tanimukai H, Grundke-Iqbal I. Tau pathology in Alzheimer disease and other tauopathies. Biochim Biophys Acta. 2005; 1739 (2–3):198–210. [PubMed: 15615638]

19. Kwiatkowski TJ Jr, Bosco DA, Leclerc AL, Tamrazian E, Vanderburg CR, Russ C, Davis A, Gilchrist J, Kasarskis EJ, Munsat T, Valdmanis P, Rouleau GA, Hosler BA, Cortelli P, de Jong PJ, Yoshinaga Y, Haines JL, Pericak-Vance MA, Yan J, Ticozzi N, Siddique T, McKenna-Yasek D, Sapp PC, Horvitz HR, Landers JE, Brown RH Jr. Mutations in the FUS/TLS gene on chromosome 16 cause familial amyotrophic lateral sclerosis. Science. 2009; 323 (5918):1205–1208. [PubMed: 19251627]

20. Li M, Makkinje A, Damuni Z. The myeloid leukemia-associated protein SET is a potent inhibitor of protein phosphatase 2A. J Biol Chem. 1996; 271 (19):11059–11062. [PubMed: 8626647]

21. Liu F, Grundke-Iqbal I, Iqbal K, Gong CX. Contributions of protein phosphatases PP1, PP2A, PP2B and PP5 to the regulation of tau phosphorylation. Eur J Neurosci. 2005; (8):1942–1950. [PubMed: 16262633]

22. Liu Z, Jang SW, Liu X, Cheng D, Peng J, Yepes M, Li XJ, Matthews S, Watts C, Asano M, Hara-Nishimura I, Luo HR, Ye K. Neuroprotective actions of PIKE-L by inhibition of SET proteolytic degradation by asparagine endopeptidase. Mol Cell. 2008; 29 (6):665–678. [PubMed: 18374643]

23. Miklossy J, Steele JC, Yu S, McCall S, Sandberg G, McGeer EG, McGeer PL. Enduring involvement of tau, beta-amyloid, alpha-synuclein, ubiquitin and TDP-43 pathology in the amyotrophic lateral sclerosis/parkinsonism-dementia complex of Guam (ALS/PDC). Acta Neuropathol. 2008; 116 (6):625–637. [PubMed: 18843496]

24. Mimuro M, Kokubo Y, Kuzuhara S. Similar topographical distribution of neurofibrillary tangles in amyotrophic lateral sclerosis and parkinsonism-dementia complex in people living in the Kii peninsula of Japan suggests a single tauopathy. Acta Neuropathol. 2007; 113 (6):653–658. [PubMed: 17277950]

25. Oyanagi K, Makifuchi T, Ohtoh T, Chen KM, van der Schaaf T, Gajdusek DC, Chase TN, Ikuta F. Amyotrophic lateral sclerosis of Guam: the nature of the neuropathological findings. Acta Neuropathol. 1994; 88 (5):405–412. [PubMed: 7847068]

26. Renton AE, Majounie E, Waite A, Simon-Sanchez J, Rollinson S, Gibbs JR, Schymick JC, Laaksovirta H, van Swieten JC, Myllykangas L, Kalimo H, Paetau A, Abramzon Y, Remes AM, Kaganovich A, Scholz SW, Duckworth J, Ding J, Harmer DW, Hernandez DG, Johnson JO, Mok K, Ryten M, Trabzuni D, Guerreiro RJ, Orrell RW, Neal J, Murray A, Pearson J, Jansen IE,

Sondervan D, Seelaar H, Blake D, Young K, Halliwell N, Callister JB, Toulson G, Richardson A, Gerhard A, Snowden J, Mann D, Neary D, Nalls MA, Peuralinna T, Jansson L, Isoviita VM, Kaivorinne AL, Holtta-Vuori M, Ikonen E, Sulkava R, Benatar M, Wuu J, Chio A, Restagno G, Borghero G, Sabatelli M, Consortium I, Heckerman D, Rogaeva E, Zinman L, Rothstein JD, Sendtner M, Drepper C, Eichler EE, Alkan C, Abdullaev Z, Pack SD, Dutra A, Pak E, Hardy J, Singleton A, Williams NM, Heutink P, Pickering-Brown S, Morris HR, Tienari PJ, Traynor BJ. A hexanucleotide repeat expansion in C9ORF72 is the cause of chromosome 9p21-linked ALS-FTD. Neuron. 2011; 72 (2):257–268.10.1016/j.neuron.2011.09.010 [PubMed: 21944779]

27. Seo SB, McNamara P, Heo S, Turner A, Lane WS, Chakravarti D. Regulation of histone acetylation and transcription by INHAT, a human cellular complex containing the set oncoprotein. Cell. 2001; 104 (1):119–130. [PubMed: 11163245]

28. Sreedharan J, Blair IP, Tripathi VB, Hu X, Vance C, Rogelj B, Ackerley S, Durnall JC, Williams KL, Buratti E, Baralle F, de Belleroche J, Mitchell JD, Leigh PN, Al-Chalabi A, Miller CC, Nicholson G, Shaw CE. TDP-43 mutations in familial and sporadic amyotrophic lateral sclerosis. Science. 2008; 319 (5870):1668–1672. [PubMed: 18309045]

29. Sternberger NH, Sternberger LA, Ulrich J. Aberrant neurofilament phosphorylation in Alzheimer disease. Proc Natl Acad Sci USA. 1985; 82 (12):4274–4276. [PubMed: 3159022]

30. Tanimukai H, Grundke-Iqbal I, Iqbal K. Inhibitors of protein phosphatase-2A: topography and subcellular localization. Brain Res Mol Brain Res. 2004; 126 (2):146–156. [PubMed: 15249138]

31. Tanimukai H, Grundke-Iqbal I, Iqbal K. Up-regulation of inhibitors of protein phosphatase-2A in Alzheimer's disease. Am J Pathol. 2005; 166 (6):1761–1771. [PubMed: 15920161]

32. Vance C, Rogelj B, Hortobagyi T, De Vos KJ, Nishimura AL, Sreedharan J, Hu X, Smith B, Ruddy D, Wright P, Ganesalingam J, Williams KL, Tripathi V, Al-Saraj S, Al-Chalabi A, Leigh PN, Blair IP, Nicholson G, de Belleroche J, Gallo JM, Miller CC, Shaw CE. Mutations in FUS, an RNA processing protein, cause familial amyotrophic lateral sclerosis type 6. Science. 2009; 323 (5918):1208–1211. [PubMed: 19251628]

33. Veeranna, Yang DS, Lee JH, Vinod KY, Stavrides P, Amin ND, Pant HC, Nixon RA. Declining phosphatases underlie aging-related hyperphosphorylation of neurofilaments. Neurobiol Aging. 2009

34. Wang X, Blanchard J, Kohlbrenner E, Clement N, Linden RM, Radu A, Grundke-Iqbal I, Iqbal K. The carboxy-terminal fragment of inhibitor-2 of protein phosphatase-2A induces Alzheimer disease pathology and cognitive impairment. FASEB J. 2010; 24 (11):4420–4432. [PubMed: 20651003]

35. Xiao S, McLean J, Robertson J. Neuronal intermediate filaments and ALS: a new look at an old question. Biochim Biophys Acta. 2006; 1762 (11–12):1001–1012.10.1016/j.bbadis.2006.09.003 [PubMed: 17045786]

36. Yu G, Yan T, Feng Y, Liu X, Xia Y, Luo H, Wang JZ, Wang X. Ser9 phosphorylation causes cytoplasmic detention of I2(PP2A)/SET in Alzheimer disease. Neurobiol Aging. 2013; 34 (7): 1748–1758.10.1016/j.neurobiolaging.2012.12.025 [PubMed: 23374587]
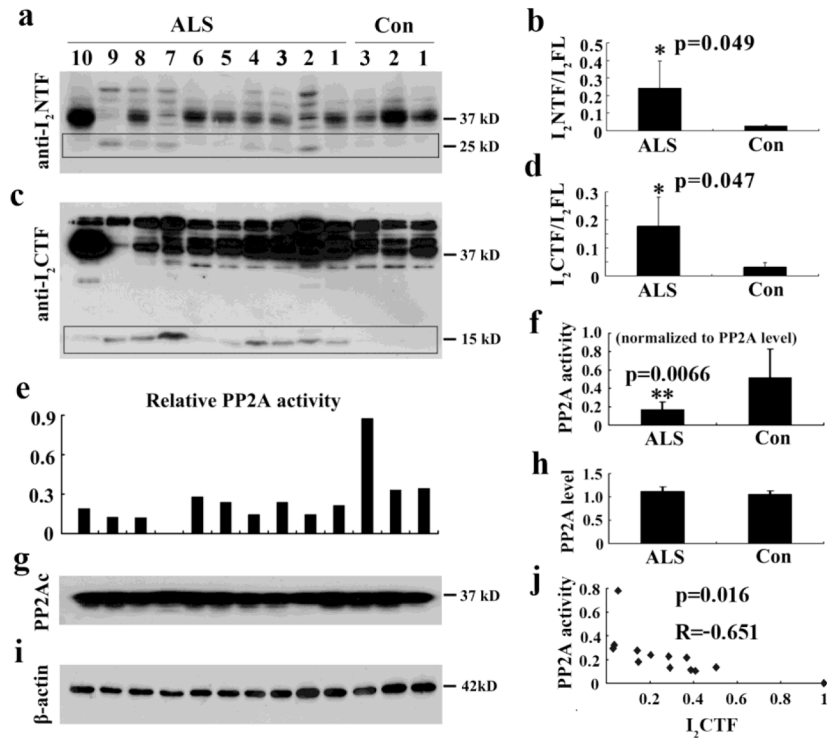
Fig. 1. I$_2^{PP2A}$ is cleaved into I$_{2NTF}$ and I$_{2CTF}$ and PP2A activity is compromised in spinal cords of sporadic ALS cases

A, C) Western blots developed with mAb to I$_{2NTF}$ and pAb to I$_{2CTF}$ show the cleavage of I$_2^{PP2A}$ in spinal cords of ten cases of sporadic ALS and three age-matched controls. B, D) Quantitative analysis of the blots shows that the cleavage of I$_2^{PP2A}$ into I$_{2NTF}$ and I$_{2CTF}$ (ratio of I$_{2NTF}$ or I$_{2CTF}$ to I$_2^{PP2A}$ full-length) is markedly increased in sporadic ALS cases as compared with control group. E, F) PP2A activity determined by the phosphatase ELISA assay is markedly decreased in ALS cases compared with control group. G, H) Western blots developed with anti-PP2Ac mouse monoclonal antibody showed no significant change in the levels of the phosphatase in ALS cases when compared with control group I) β-actin as a loading control. J) PP2A activity inversely correlated to the level of I$_{2CTF}$ in the spinal cord. I$_{2FL}$ = I$_2^{PP2A}$ full-length.
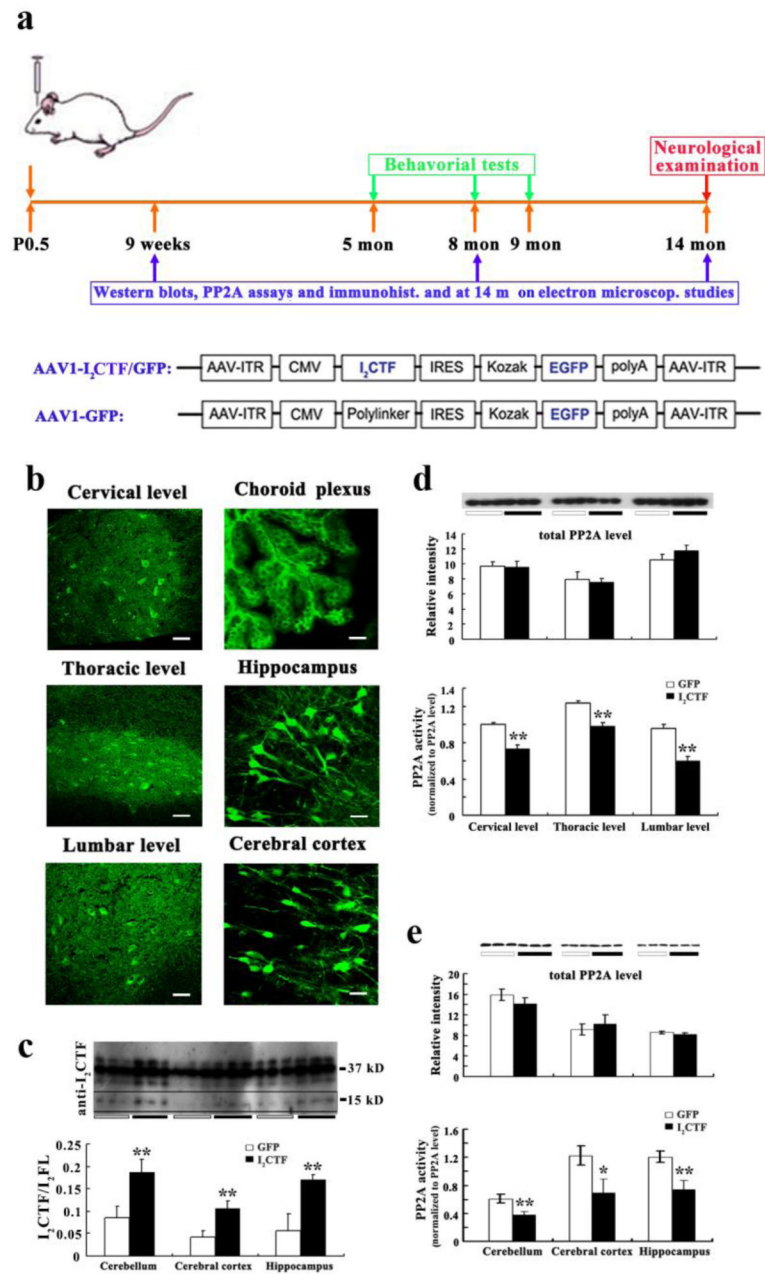
Fig. 2. AAV1-mediated gene expression of I$_{2CTF}$ inhibits PP2A activity without affecting the expression of the PP2A catalytic subunit PP2Ac in the brain and the spinal cord of rats
a: Study design and linear maps of the AAV vector plasmids (based on pTRUF12) employed. With the exception of the inverted terminal repeats (ITR), all viral genes had been removed and replaced with GFP or I$_{2CTF}$ and GFP. CMVe-CBA (cytomegalovirus enhancer-chicken beta actin promoter); IRES (internal ribosomal entry site) from poliovirus; **b:** Immunohistofluorescence with anti-GFP showed transduction of both brain and spinal cord; scale bars in cervical level, thoracic level and lumber level: 75 μm; scale bars in choroid plexus, hippocampus and cerebral cortex: 50 μm. **c:** Western blots developed with pAb to I$_{2CTF}$ showed a marked increase in the brain level of I$_{2CTF}$ in AAV1-I$_{2CTF}$ animals. **d and e:** Immunoprecipitation of PP2A from spinal cord **(d)** and brain **(e)** with rabbit

polyclonal R123d anti-PP2Ac, followed by phosphatase activity assays showed inhibition of PP2A activity in I_{2CTF} rats. **b–e:** Data from 14-month-old rats. *p<0.05; **p<0.01. Scale bar in b: cervical level, thoracic level and lumbar level, 75 μm; choroid plexus, hippocampus and cerebral cortex, 50 μm. $I_{2FL} = I_2^{PP2A}$ full-length.
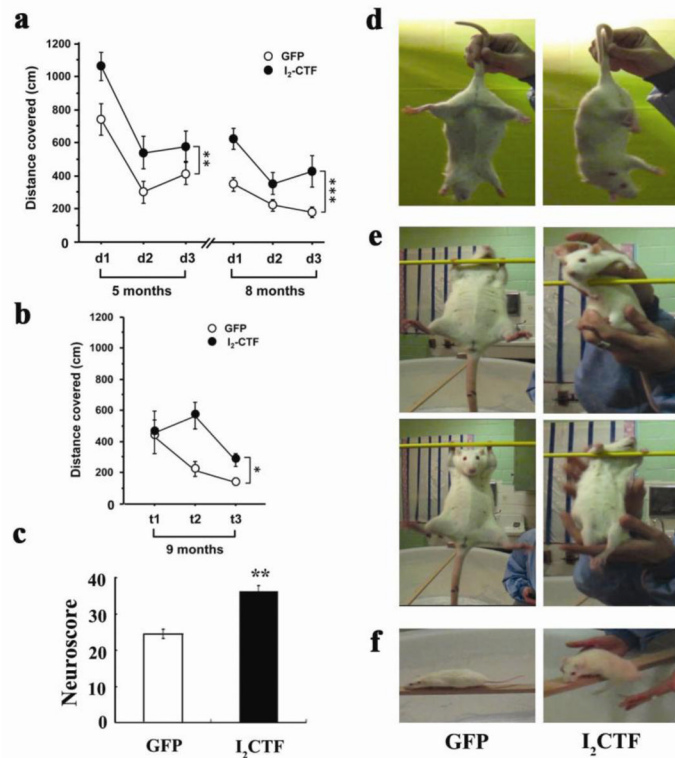
Fig. 3. I₂CTF expression induces spatial reference memory and neurological and motor impairments

a. Compared to GFP control (n=7), I$_{2CTF}$ (n=8) rats showed impairment in spatial reference memory at 5 (p=0.005) and at 8 (p<0.001) months of age in Morris Water Maze task and **b.** in long-term spatial reference memory examined one month later (at 9 months of age) by transfer task in the water maze (p=0.041). d=day; t=trial; asterisks refer to statistical difference between the two curves and not any single time point; *p<0.05; **p<0.01 and ***p<0.001. **c:** I$_{2CTF}$ rats (n=8) presented a higher neuroscore than GFP rats (n=7), reflecting a robust neurological impairment; **d:** I$_{2CTF}$ rats displayed severe muscle atrophy, inducing abnormal posture and hind limb clasping; **e:** weakness in prehensile strength; and **f:** disability in walking.
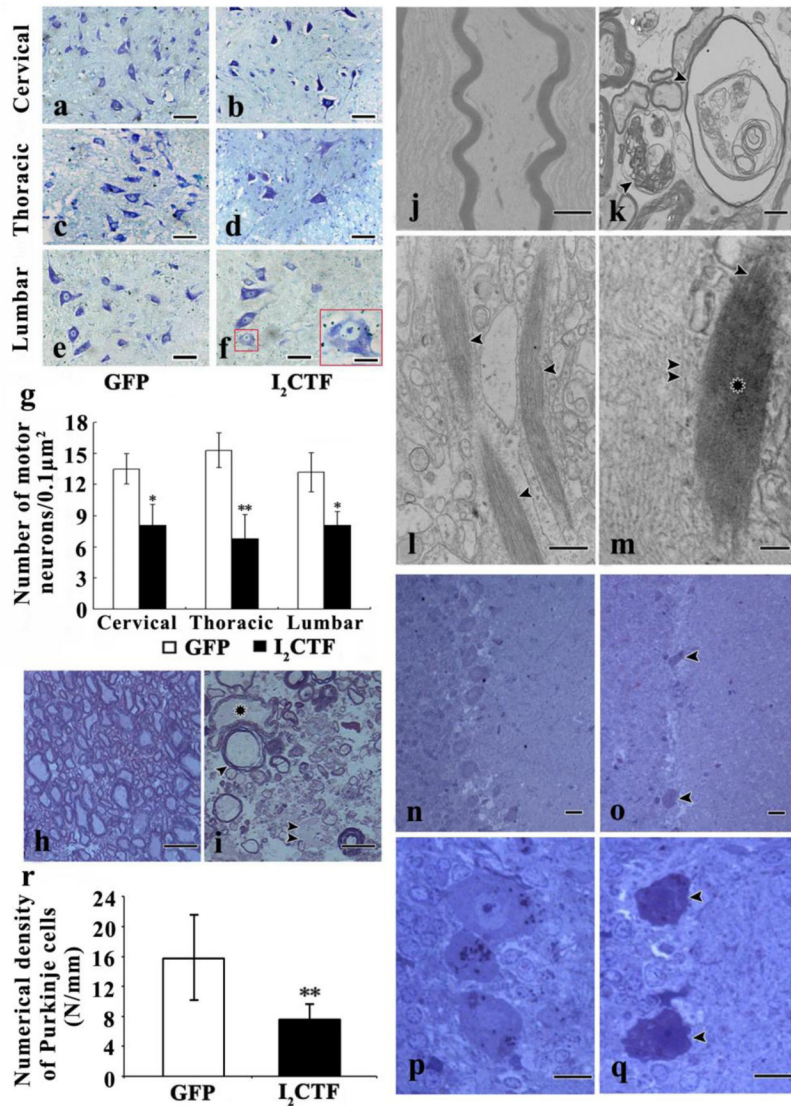
Fig. 4. I$_{2CTF}$ expression induces degeneration and loss of motor neurons, and degeneration and demyelination of axons, proliferation of neurofilaments, accumulation of tight fibrous bundles in the neuronal soma and axons at all levels of the spinal cord, and loss of Purkinje cells in the cerebellum

a–g: Nissl staining showed condensation (a–f), spongiosis (f) and loss (g) of motor neurons in the spinal cords of I$_{2CTF}$ rats. **h (GFP rats), i (I$_{2CTF}$ rats):** Toluidine blue-stained sections of the epon-embedded spinal cord showed a severe degeneration (i, asterisk), demyelination (i, arrowhead), and residues of degraded axons (i, double arrowheads) in I$_{2CTF}$ rats; **j–m:** Electron microscopy showed normal axons in GFP rats (j), and degenerated and demyelinated axons (k, arrowheads),inclusions of compact fibrous bundles in neuronal processes (l, arrowhead), 20–35 nm thick filaments in compact fibrous bundles (m, arrowhead) compared to ~10 nm neurofilaments (double arrowheads) and loss of morphology of fibers in the central portion of inclusions (m, asterisk). **n–q:** Toluidine blue-stained sections of the epon-embedded tissue showed an extensive cerebellar degeneration associated with cytoplasmic condensation and loss of Purkinje cells (o, q, arrowhead) in the I$_{2CTF}$ rats. n, p: GFP rats. **r:** quantitation of the numerical density of Purkinje cells from cresyl violet stained paraffin sections of cerebellar cortices from I$_{2CTF}$ and GFP rats. **a–r:**

Data from 14-month-old rats. **g, r:** The data are presented as mean±SD. Scale bar: a–f: 50 μm; f: bar in inset: 10 μm; g, h: 15 nm; m, n: 50 nm; o, p: 25 nm; i, j: 2 μm; k: 500 nm; l: 100 nm.
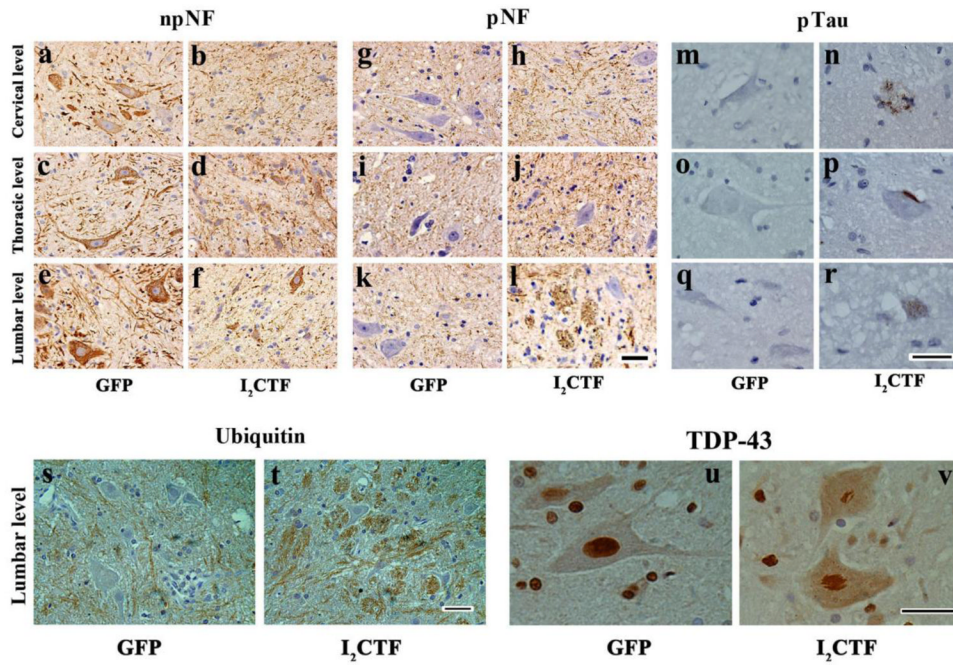
Fig. 5. I$_{2CTF}$ expression induces hyperphosphorylation and accumulation of neurofilaments and tau, increase in the expression of ubiquitin, and aggregation and translocation of TD43 from the motor neuronal nucleus to the cytoplasm in I$_{2CTF}$ rats
a–f: Immunohistochemical staining with anti-non-phosphorylated (np) NF-H mAb (SMI33) showed a decrease in the density of npNF-H-positive motor neurons in the spinal cords of I$_{2CTF}$ rats; **g–l:** Immunohistochemical staining with anti-phospho (p) NF-H mAb (SMI34) showed an increase in phosphorylation and accumulation of neurofilaments in the axonal tracts of the spinal cords of I$_{2CTF}$ rats; **m–r:** Immunohistochemical staining with anti-pSer262/356 tau (mAb 12E8) showed abnormal hyperphosphorylation and aggregation of tau in the motor neuron cell cytoplasm reminiscent of stage 0 (r) and stage 1 (p) neurofibrillary tangles, and in dystrophic neurites resembling neuritic plaques (n); **s–t:** An increase in ubiquitin immunostaining was evident in the axonal tracts in the spinal cords of I$_{2CTF}$ rats; and **u–v:** Immunohistochemical staining showed condensation and translocation of TDP43 from the motor neuron nucleus to the cytoplasm in the spinal cords of I$_{2CTF}$ rats. **a–v**: Data from 14-month-old rats. Scale bar: 25 μm.
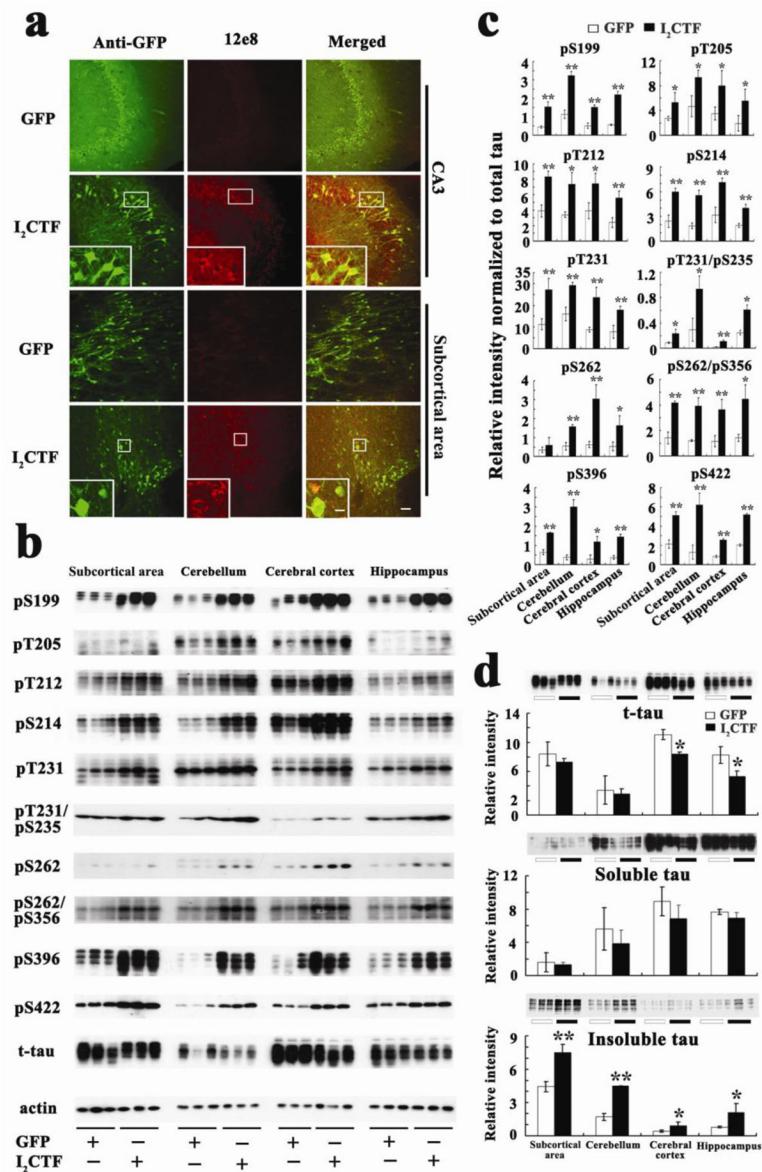
Fig. 6. Expression of I$_{2CTF}$ induces increase in abnormal hyperphosphorylation and accumulation of sarkosyl-insoluble tau in the brains of I$_{2CTF}$ rats
a: Immunohistofluorescent staining showed abnormal hyperphosphorylation of tau at pSer262/356 (12E8 site) in the CA3 and the subcortical area (SA) of I$_{2CTF}$ rats; **b:** Western blots and **c:** quantitative analysis showed a reduction in the level of total tau and an increase in the abnormal hyperphosphorylation of tau at multiple AD pathological sites and **d:** increase in sarkosyl-insoluble tau in the I$_{2CTF}$ rats' hippocampus, cerebral cortex, subcortical area (SA) and cerebellum. **a–e**: Data from 14-month-old rats. Scale bar: a: 100 μm; inset: 25 μm.
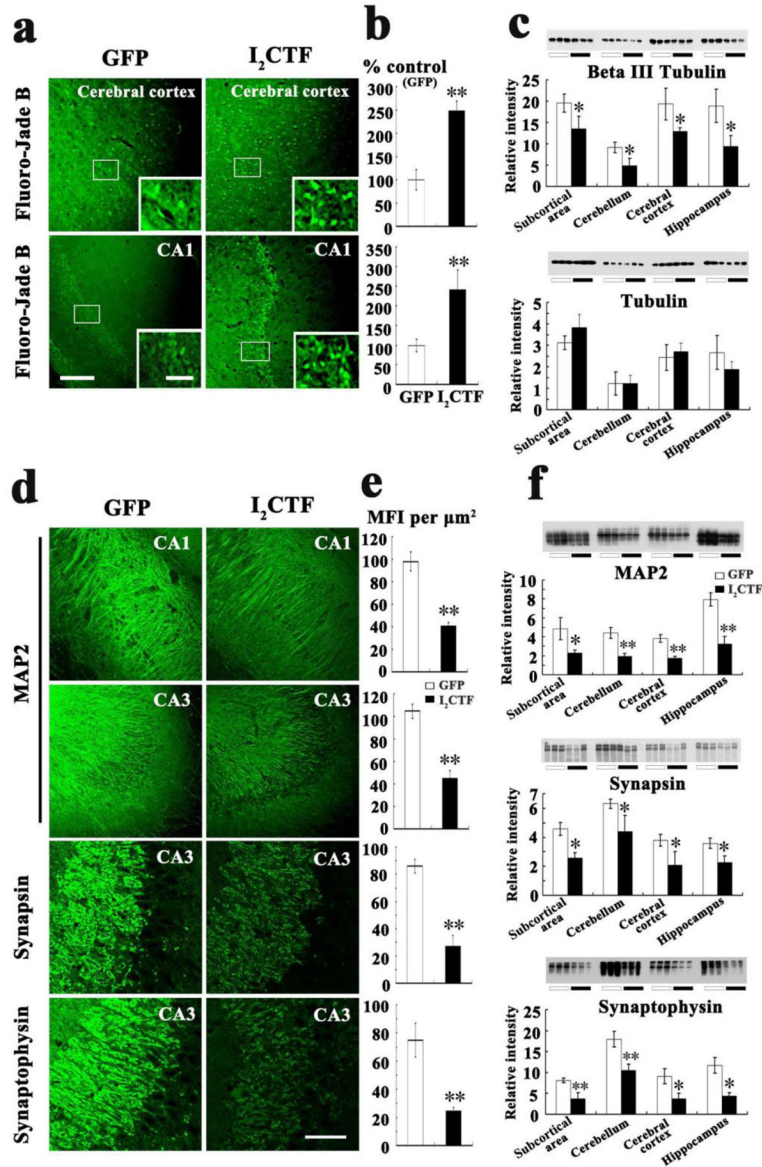
Fig. 7. Expression of I$_{2\text{CTF}}$ causes neurodegeneration and loss of neuronal plasticity
a, b: Fluoro-Jade B staining showed an increase in neurodegeneration in I$_{2\text{CTF}}$ rats; **c:** Western blots and their quantitative analysis showed a decrease in the level of βIII tubulin and not in total tubulin in I$_{2\text{CTF}}$ rats; **d, e:** Immunohistofluorescent staining showed a decrease in the density of MAP2 in CA1 and CA3, synapsin 1 in CA3, and synaptophysin in CA3 of the hippocampi of I$_{2\text{CTF}}$ rats; and **f:** Western blots and their quantitative analysis showed a marked decrease in the levels of MAP2, synapsin 1, and synaptophysin in the I$_{2\text{CTF}}$ rats' hippocampus, cerebral cortex, subcortical area (SA) and cerebellum. Data from 14-month-old rats. *p<0.05; **p<0.01. Scale bar: a: 300 μm; inset: 100 μm; d: 500 μm.
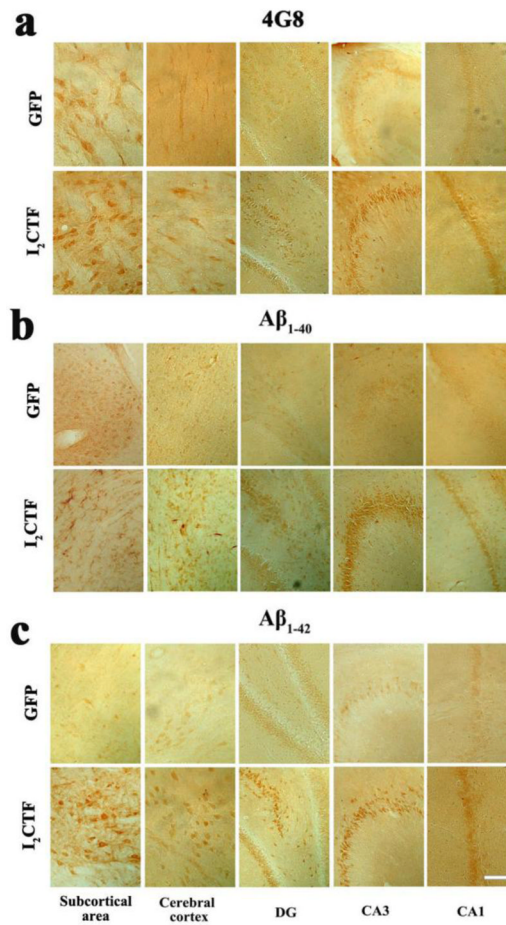
Fig. 8. I$_{2CTF}$ causes increase in the expression of Aβ$_{1-40}$ and Aβ$_{1-42}$ in the brain
Immunohistochemical staining showed an increase in the expression of Aβ as detected by **a:** anti-Aβ/APP (4G8), **b:** anti-Aβ$_{1-40}$, and **c:** anti-Aβ$_{1-42}$ in CA1, CA3, and dentate gyrus in the hippocampus, cerebral cortex, and in the subcortical area (SA) of I$_{2CTF}$ rats. Data from 14-month-old rats. Scale bar: a–c: 300 µm.